DOI 10.2478/ama-2025-0012

AN OPTIMAL BRAKING FORCE DISTRIBUTION IN THE RIGID DRAWBAR TRAILERS WITH TANDEM SUSPENSION

Zbigniew KAMIŃSKI*

*Faculty of Mechanical Engineering, Bialystok University of Technology, ul. Wiejska 45C, 15-351 Białystok, Poland

z.kaminski@pb.edu.pl

received 15 November 2023, revised 11 November 2024, accepted 15 November 2024

Abstract: Rigid drawbar agricultural trailers with laden weight of up to 13 tonnes have a single axle, up to 19 tonnes tandem axles. Carried out analysis of a tractor semi-mounted trailer combination showed that under ideal braking, the adhesion utilised by all axles and a coupling device are equal. By adopting the concept of treating the coupling device as a conventional front axle, the requirements of EU Directive 2015/68 for multi-axle trailers have been used to develop a new method for selecting the brake force distribution of semi-trailers with different suspensions. First, the forces acting on a single and tandem semi-trailer were analysed during braking. An algorithm based on the quasi-Monte Carlo method was then proposed to solve the constrained optimisation of the linear brake force distribution of semi-trailers equipped with ALB or MLB regulators. Finally, examples of MATLAB calculations were given for a 5 tonne single axle trailer and a 16-tonne trailer with 5 different tandem suspensions: bogie, two leaf spring, two leaf spring and rods, two leaf spring with dynamic equalisation and air spring. The results of the work are expected to provide a reference for the design and evaluation of the braking system of agricultural semi-trailers, especially with different types of tandem axles, to improve braking performance and reduce coupling forces.

Key words: agriculture tractor/semi-trailer combination, tandem axle, air braking system, braking force distribution, optimization

1. INTRODUCTION

The design of the running gear of agricultural trailers with rigid (unbalanced) drawbar depends on their load capacity. Semi-mounted trailers with laden weight of up to 13 tonnes have a single axle, up to 19 tonnes tandem axles and up to 22.5 tonnes triaxle [1]. A multiple-axle unit consists of axles spaced closely together, usually between 1.2 m and 1.85 m [2, 3]. Tandem and triple axles are used to increase the vehicle's load capacity and load distribution between the axles, regardless of road surface irregularities [4]. Generally, two basic tandem suspension arrangements have been developed: a central pivoting single vertical semi-elliptic or parabolic spring which has an axle clamped to it at either end and a pivoting reactive or non-reactive balance beam which interconnects adjacent first and second semi-elliptic springs via their shackle plates [5-7].

During a brake application, all the vehicles of a combination tractor-trailer should be braked with similar intensity to enable efficient deceleration without the risk of the combination losing its directional stability. From 2016, EU legislation on agricultural vehicles [8] has required agricultural trailers travelling at speeds above 30 km/h to comply with the same braking efficiency of 50% as commercial trailers [9]. Furthermore, agricultural balanced trailers with a total mass exceeding 3500 kg (categories R3 and R4) require a specific brake force distribution among the axles. As in the case of commercial vehicles [9], the individual parts of the combination are treated as individual vehicles, so that the coupling interactions between them are not taken into account. No recommendations are made in this respect for semi-trailers. To share the brake force distribution between a tractor and a towed vehicle, permissible compatibility corridors for the braking rate of the tractor and the towed vehicle refer to the pressure values of the control line between these vehicles that have been introduced. The compliance with compatibility requirements, as well as requirements regarding high-speed operation (response time of less than 0.6 s [8]), contribute to the shortening of stopping distance of tractor-trailer combinations and the reduction of forces in the coupling during emergency braking [10]. The implementation of the new European legislation in the field of agricultural vehicles places high demands on the manufacturers of agricultural trailers, tractors and machines concerning braking systems [11].

Most of the works on agricultural trailer braking deal with various aspects of the braking process of tractor-trailer combinations, mainly with two-axle trailers [12-14]. Papers [15, 16], describe the braking mechanics of a tractor with a single-axle trailer while moving up and down a slope under various operating conditions. The dynamic behaviour during braking of tractor-semitrailer combinations in terms of stability and road safety has been analysed in [17] and [18]. Paper [19], on the other hand, describes the braking of a semitrailer endowed with an inertial braking system, working in aggregate with the tractor. Both the theoretical and practical aspects of the braking performance of tractor-semitrailer combinations were examined in [20] and [21]. To simplify the theoretical considerations in [20], the tandem bogie suspension was replaced by a single axle and the forces from the wheels were applied to the bogie joint without considering the interaction between the tandem axles. From the designer's (manufacturer's) point of view, any analysis of the braking mechanics of a tractor-trailer combination seems to be of little use for the design of semi-trailer braking systems, as it requires

specific assumptions to be made about the geometric and mass parameters of a farm tractor. Moreover, these considerations usually apply to single-axle semi-trailers but not to semi-trailers with tandem suspension. And as is well known [3, 4, 22], when a braking force is applied on a tandem axle, there is often a load transfer among the axles, and the lighter loaded axle tends to lock up before the other. This phenomenon, which is dependent on the tandem suspension type used, harms braking performance and directional stability. If the lock-up occurs on the trailing axle, it can lead to a complete loss of directional stability [3]. Therefore, in this study, the influence of inter-axle load transfer in semitrailers with different tandem suspensions has been considered in the development of the brake force distribution methodology for use by designers and manufacturers of agricultural machinery, thus filling a gap in the literature.

The design process of a new brake system starts with the selection of the distribution of brake forces [23]. The axle load transfer and braking force distribution play an important role in the safety and dynamic stability of road vehicles [24, 25]. In general, for the correct design of a vehicle braking system, it is essential to know the ideal brake force distribution between the axles for laden and unladen vehicles [26]. With the braking distribution at the ideal level, the braking performance is maximized, and the brake stability is then also guaranteed [27]. The optimum braking condition is achieved when each axle has the same utilised adhesion, i.e. the ratio between the braking force on each axle and its vertical load is the same [28, 29]. Under such conditions, the ratio of the longitudinal force and vertical force on the coupling device is also the same [30].

This latter condition became an inspiration to use the brake force distribution strategy for two-axle trailers, according to the EU regulations [8], to determine the braking force distribution in semi-trailers between the axle unit (single or tandem) and the coupling device that attaches the towed vehicle to the farm tractor. With this approach, a semi-trailer can be considered as if it were an individual braked vehicle with braking forces at the axle wheels and the coupling device.

To calculate the brake distribution of a single-axle semi-trailer, the analytical method can be used as for two-axle trailers [31, 32]. However, for tandem semitrailers, the analysis is more complicated because the leading and trailing axle loads are functions of the trailer load and the type and geometry of the tandem axle unit [4]. Therefore, even for vehicles with the simplest of tandem suspensions, such as a walking beam and bogie [31, 33] or a double elliptic leaf spring suspension [34], optimisation methods are used to calculate and select the brake force distribution. To find an optimal linear force distribution, which is mostly used in trailer air brake systems due to the linear characteristics of the brake force regulators, the quasi-Monte Carlo method was used in this paper.

The remainder of the paper is structured as follows: in section 2, the equations of forces acting during braking on a tractor single-axle semi-trailer and a tractor tandem-axle semi-trailer combination are developed to find the condition of ideal braking force distribution; in section 3, the analysis of the forces acting during braking on a semi-trailer with different types of tandem suspension is presented; in section 4, the UE regulations for the brake force distribution adapted to semi-trailers are described; in section 5, the quasi Monte Carlo method and the algorithm of linear brake force distribution are described. The results of optimising the different tandem axles are analysed and discussed in section 6. Finally, a summary and conclusions are drawn in Section 7.

The findings of the work are expected to provide a reference for the design and evaluation of the air braking system of agricultural semi-trailers, especially with different types of tandem axles, to improve braking performance and reduce coupling forces.

2. IDEAL BRAKING OF TRACTOR AND SEMI-TRAILER

Tractor-semitrailer combination is modelled as two rigid body hinges to each other, and suspension deflection is ignored. The forces acting on a braking farm tractor with single and tandem axle semi-trailers are shown in Figures 1-3. For simplicity, it is assumed that aerodynamic and rolling drag is neglected.

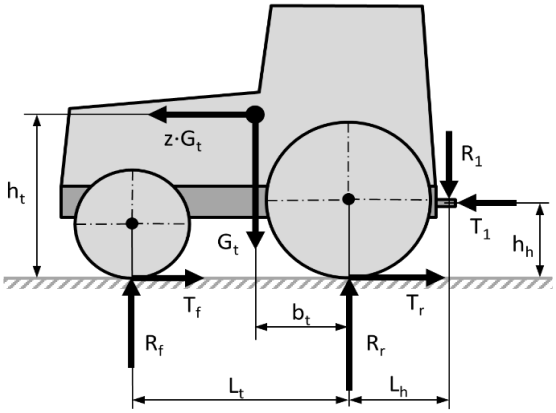

Fig. 1. Forces acting on a farm tractor (ISO coordinate system [35])

Using the notation from Fig. 1, the equations of forces and moments exerted on the decelerating tractor are of the form:

$$\sum X = z \cdot G_t + T_1 - T_f - T_r = 0 \tag{1}$$

$$\sum Z = R_f + R_r - G_t - R_1 = 0 \tag{2}$$

$$\sum M_1 = -R_f(L_t + L_h) - R_r L_h + G_t(L_h + b_t) + z \cdot G_t(h_t - h_h) + (T_f + T_r)h_h = 0 \tag{3}$$

where: T_f, T_r – front and rear axle braking forces, R_f, R_r – axle loads, T_1, R_1 – horizontal and vertical force on the coupling, L_t – inter-axle spacing, b_t – distance between centre of gravity and rear axle, h_t – height of the centre of gravity, L_h – distance from coupling device to the rear axle, G_t – trailer weight, z – braking rate.

The equilibrium equations of forces and moments exerted on the single-axle semi-trailer shown in Fig. 2 are as follows:

$$\sum X = z \cdot G - T_1 - T_{21} = 0 \tag{4}$$

$$\sum Z = R_1 + R_{21} - G = 0 \tag{5}$$

$$\sum M_1 = R_{21}L_1 - G \cdot a + z \cdot G(h - h_h) + T_{21}h_h = 0 \tag{6}$$

where: T_2 – axle brake force, R_{21} – axle load, L_1 – distance between coupling device and semi-trailer's axle, a – distance from the coupling to the centre of gravity, h – height of the centre of gravity, G – trailer weight.

From the equations (2) and (5) of vertical forces (after elimination of the reaction R_1) and the equation of moments for the tractor (3) and the trailer (6) concerning the coupling, the vertical reactions are obtained:

$$R_f = \frac{G_t}{L_t}[b_t + z(h_t - h_h)] + (T_f + T_r)\frac{h_h}{L_t} - R_1\frac{L_h}{L_t} \tag{7}$$

DOI 10.2478/ama-2025-0012

$$R_r = \frac{G_t}{L_t}[L_t - b_t - z(h_t - h_h)] - \left(T_f + T_r\right)\frac{h_h}{L_t} + R_1\frac{L_h+L_t}{L_t} \tag{8}$$

$$R_1 = \frac{G}{L_1}[L_1 - a + z(h - h_h)] + T_{21}\frac{h_h}{L_1} \tag{9}$$

$$R_{21} = \frac{G}{L_1}[a - z(h - h_h)] - T_{21}\frac{h_h}{L_1} \tag{10}$$

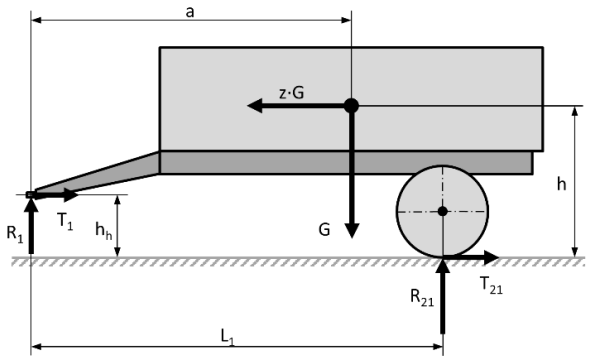

Fig. 2. Forces acting on a single-axle semi-trailer

In the case of ideal braking of a tractor with a single-axle semi-trailer, the adhesion utilisation of each axle is the same and equal to the braking rate of the combination, i.e. f_f=f_r=f_{21}=z. Hence T_f+T_r=z(R_f+R_r) and T_{21}=z·R_{21}. Then the ground reactions to the axle wheels are as follows:

$$R_f = \frac{G_t(b_t+z\cdot h_t)-G(L_h-z\cdot h_h)}{L_t} + \frac{G[a-z(h-h_h)](L_h-z\cdot h_h)}{L_t(L_1+z\cdot h_h)} \tag{11}$$

$$R_r = G_t + R_1 - R_f \tag{12}$$

$$R_1 = \frac{G[L_1-a+z\cdot h]}{L_1+z\cdot h_h} \tag{13}$$

$$R_{21} = \frac{G[a-z(h-h_h)]}{L_1+z\cdot h_h} \tag{14}$$

So that during ideal braking, the ratio of the tangential force to the vertical force acting on the coupling:

$$f_1 = \frac{T_1}{R_1} = \frac{z\cdot G - T_{21}}{G - R_{21}} = z \tag{15}$$

is the same as the braking rate of the vehicle combination.

The system of equilibrium equations for a braked single-axle semi-trailer with walking beam tandem suspension (Fig. 3) is given as:

$$\sum X = z\cdot G - T_1 - T_{21} - T_{22} = 0 \tag{16}$$

$$\sum Z = R_1 + R_{21} + R_{22} - G = 0 \tag{17}$$

$$\sum M_1 = R_{21}L_1 + R_{22}(L_1 + L_2) - G\cdot a + z\cdot G(h - h_h) + (T_{21} + T_{22})h_h = 0 \tag{18}$$

where: L_2 – tandem axle spread.

From the equations (2), (17) of vertical forces (after elimination of the reaction R_1) and the equation of moments for the tractor (3) and the trailer (18) with respect to the coupling and the relationship between the reactions in the tandem suspension:

$$\sum M_2 = R_{22}d_2 - R_{21}d_1 + (T_{21} + T_{22})h_s = 0 \tag{19}$$

vertical reactions are obtained:

$$R_f = \frac{G_t}{L_t}[b_t + z(h_t - h_h)] + \left(T_f + T_r\right)\frac{h_h}{L_t} - R_1\frac{L_h}{L_t} \tag{20}$$

$$R_r = \frac{G_t}{L_t}[L_t - b_t - z(h_t - h_h)] - \left(T_f + T_r\right)\frac{h_h}{L_t} + R_1\frac{L_h+L_t}{L_t} \tag{21}$$

$$R_1 = \frac{G}{L}[L - a + z(h - h_h)] - (T_{21} + T_{22})\frac{(h_s - h_h)}{L} \tag{22}$$

$$R_{21} = G[a - z(h - h_h)]\frac{d_2}{L_2 L} + \frac{T_{21}+T_{22}}{L_2 L}[(L_1 + L_2)h_s - d_2 h_h] \tag{23}$$

$$R_{22} = G[a - z(h - h_h)]\frac{d_1}{L_2 L} - \frac{T_{21}+T_{22}}{L_2 L}[L_1 h_s + d_1 h_h] \tag{24}$$

where: d_1 and d_2 – beam length, h_s – height of support position, $L_2 = d_1 + d_2$ and $L = L_1 + d_1$.

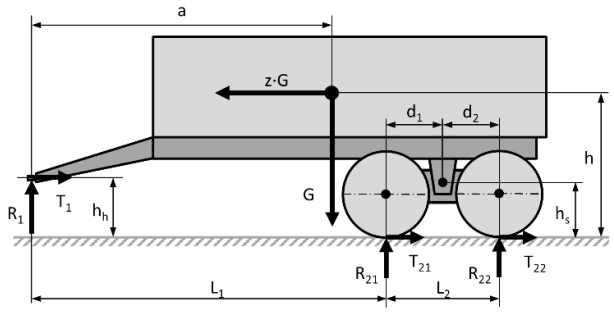

Fig. 3. Forces acting on a tandem-axle semi-trailer

During ideal braking of the combination of tractor-semitrailer with tandem suspension, the adhesion utilisation of each axle is the same and equal to the braking rate: f_f=f_r=f_{21}=f_{22}=z, which means T_f+T_r=z(R_f+R_r) and T_{21}+T_{22}=z(R_{21}+R_{22}). Then, the vertical reactions at the coupling and the wheels of the trailer are as follows:

$$R_1 = \frac{G[L-a+z(h-h_s)]}{L-z(h_s-h_h)} \tag{25}$$

$$R_{21} = \frac{G[a-z(h-h_h)](d_2+z\cdot h_s)}{L_2[L-z(h_s-h_h)]} \tag{26}$$

$$R_{22} = \frac{G[a-z(h-h_h)](d_1-z\cdot h_s)}{L_2[L-z(h_s-h_h)]} \tag{27}$$

The quotient of the tangential force to the vertical force on the coupling:

$$f_1 = \frac{T_1}{R_1} = \frac{z\cdot G-(T_{21}+T_{22})}{G-(R_{21}+R_{22})} = z \tag{28}$$

is therefore the same as the adhesion utilisation rate for each axle of the vehicle combination. Similar calculations can be carried out for other types of tandem suspensions, also considering unsprung mass, with the same results. Identical results shall be obtained for the ideal braking conditions of the tractor-trailer combination [30].

Thus, the ideal braking condition is unambiguously defined and to determine the ground reaction and then the distribution of braking forces, it is not necessary to analyse the braking process of the entire combination - only the braking process of the trailer alone may be considered.

sciendo
DOI 10.2478/ama-2025-0012

3. BRAKING OF SEMI-TRAILERS WITH TANDEM SUSPENSION

A rigid two-dimensional model is used to analyse the brake force distribution of tandem-axle semitrailers (Fig. 3). The braking forces T_{21} and T_{22} of tandem axle are considered to be known functions of the brake line pressure [8, 36]. This model also allows the use of tandem suspensions of a different type and geometry. The model equations (16)-(18) must be completed with an extra relationship between reactions R_{21} and R_{22}, determined from the equilibrium equations for a specific type of tandem suspension.

3.1. Walking beam and bogie suspension

The simplest form of tandem unit is a walking (rigid) beam [37] mounted pivotally to a frame hanger on either side of the vehicle (Fig. 4-a). In the bogie suspension [38], parabolic tapered springs are anchored upside down to the trailer frame in place of walking beams (Fig. 4-b).

The forces exerted on the walking beam and bogie suspension during braking are shown in Fig. 4.

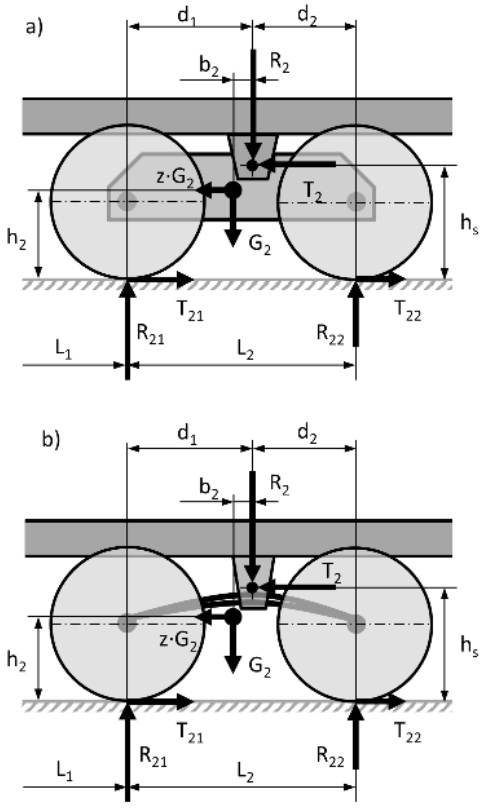

Fig. 4. Forces acting on a walking beam (a) and bogie suspension (b)

The same equilibrium force and moment equations can be used to describe both tandem suspensions:

$$\sum X = z \cdot G_2 - T_{21} - T_{22} + T_2 = 0 \tag{29}$$

$$\sum Z = R_{21} + R_{22} - R_2 - G_2 = 0 \tag{30}$$

$$\sum M_2 = R_{22}d_2 - R_{21}d_1 + G_2 b_2 - z \cdot G_2(h_s - h_2) + (T_{21} + T_{22})h_s = 0 \tag{31}$$

where: T_2 and R_2 – horizontal and vertical forces in the single-point support between the suspension and trailer frame, d_1 and d_2 – beam (parabolic spring) length, h_s – height of position, b_2 – distance of centre of unsprung weight from a support, h_2 – height of centre of unsprung weight, G_2 – unsprung weight.

By solving the system of equations (17), (18) and (31) together, considering from equation (16) that $T_{21} + T_{22} = z \cdot G - T_1$, the dynamic axle loads and the vertical coupling force during braking of semi-trailer are obtained:

$$R_1 = G\left(1 - \frac{a}{L} + z\frac{h-h_h}{L}\right) - G_2\left(\frac{b_2}{L} - z\frac{h_s-h_2}{L}\right) - (T_{21} + T_{22})\frac{h_s-h_h}{L} \tag{32}$$

$$R_{21} = \left[G\left(\frac{a}{L} - z\frac{h-h_h}{L}\right) - (T_{21} + T_{22})\frac{h_h}{L}\right]\frac{d_2}{L_2} + \left[G_2\left(\frac{b_2}{L} - z\frac{h_s-h_2}{L}\right) + (T_{21} + T_{22})\frac{h_s}{L}\right]\frac{L_1+L_2}{L_2} \tag{33}$$

$$R_{22} = \left[G\left(\frac{a}{L} - z\frac{h-h_h}{L}\right) - (T_{21} + T_{22})\frac{h_h}{L}\right]\frac{d_1}{L_2} - \left[G_2\left(\frac{b_2}{L} - z\frac{h_s-h_2}{L}\right) + (T_{21} + T_{22})\frac{h_s}{L}\right]\frac{L_1}{L_2} \tag{34}$$

where: $L_2 = d_1 + d_2$ is the tandem wheelbase and $L = L_1 + d_1$ is the trailer wheelbase.

3.2. Two leaf spring suspension

In tandem leaf spring suspension, the two most common spring types are the double eye leaf spring and the slipper spring. For agricultural trailers, the second type is more common [37-39]. The front eye of both the leading and trailing springs are hinged directly to the front hanger bracket and the levelling beam, respectively, through pin joints (Fig. 5). The rear end of the springs is captured in the equalizer beam or rear hanger.

The forces applied to the two leaf spring suspensions with two unsprung weights are illustrated in Fig. 5.

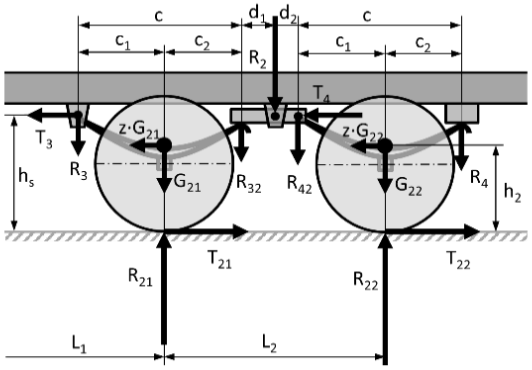

Fig. 5. Forces acting on a two leaf spring suspension

For the unsprung weight G_{21}, the following force and moment equilibrium equations are applicable:

$$\sum X = z \cdot G_{21} - T_{21} + T_3 = 0 \tag{35}$$

$$\sum Z = R_{21} - R_3 - R_{32} - G_{21} = 0 \tag{36}$$

$$\sum M_3 = -R_{32}c + R_{21}c_1 - G_{21}c_1 - z \cdot G_{21}(h_s - h_2) + T_{21}h_s = 0 \tag{37}$$

DOI 10.2478/ama-2025-0012

The equations of the balance of forces and moments for the unsprung weight of the G_{22} suspension are given by:

$$\sum X = z \cdot G_{22} - T_{22} + T_4 = 0 \tag{38}$$

$$\sum Z = R_{22} - R_4 - R_{42} - G_{22} = 0 \tag{39}$$

$$\sum M_4 = R_{42}c - R_{22}c_2 + G_{22}c_2 - z \cdot G_{22}(h_s - h_2) + T_{22}h_s = 0 \tag{40}$$

Equations (37) and (40) give the reactions at the equalizer beam ends:

$$R_{32} = (R_{21} - G_{21})\frac{c_1}{c} - z \cdot G_{21}\frac{h_s - h_2}{c} + T_{21}\frac{h_s}{c} \tag{41}$$

$$R_{42} = (R_{22} - G_{22})\frac{c_2}{c} + z \cdot G_{22}\frac{h_s - h_2}{c} - T_{22}\frac{h_s}{c} \tag{42}$$

After substitution of the expressions (41) and (42) into the equilibrium equation of the force moments on the equalizer beam:

$$R_{32}d_1 = R_{42}d_2 \tag{43}$$

a new relationship is obtained which, together with equations (17) and (18), forms a system of 3 equations which makes it possible to determine the dynamic axle loads and the vertical coupling force during braking of the semi-trailer:

$$R_1 = G - \frac{L_2}{MN}\Big\{[G[a - z(h - h_h)] - (T_{21} + T_{22})h_h]\,\frac{c_1(d_1 - d_2) + c \cdot d_2}{L_2} + G_{21}d_1[c_1 + z(h_s - h_2)] - G_{22}d_2[c_2 - z(h_s - h_2)] - (T_{21}d_1 + T_{22}d_2)h_s\Big\} \tag{44}$$

$$R_{21} = \frac{L_1 + L_2}{MN}\Big\{[G[a - z(h - h_h)] - (T_{21} + T_{22})h_h]\,\frac{d_2(c - c_1)}{L_1 + L_2} + G_{21}d_1[c_1 + z(h_s - h_2)] - G_{22}d_2[c_2 - z(h_s - h_2)] - (T_{21}d_1 + T_{22}d_2)h_s\Big\} \tag{45}$$

$$R_{22} = \frac{L_1}{MN}\Big\{[G[a - z(h - h_h)] - (T_{21} + T_{22})h_h]\,\frac{c_1d_1}{L_1} - G_{21}d_1[c_1 + z(h_s - h_2)] + G_{22}d_2[c_2 - z(h_s - h_2)] + (T_{21}d_1 + T_{22}d_2)h_s\Big\} \tag{46}$$

where: $MN = c_2d_2L_1 + c_1d_1(L_1 + L_2)$.

3.3. Two leaf–two rod suspension

Another version of the tandem axle configuration uses only two springs with slipper ends. Vertical forces are transmitted to the trailer frame via the front and rear hanger brackets and equalizer beam (according to the BPW equalising beam) [37-39].
Longitudinal forces are transferred by connecting the radius rods between the axles and the front and middle hanger brackets (Fig. 6). The parameters α_1 and α_2, as well as h_{r1} and h_{r2}, have a significant effect on the operation of the suspension. This design uses a reduced radius rod angle α_2 and a reduced pivot height h_{r2} on the rear axle to decrease inter-axle load transfer during braking [22].

The force and moment equations for unsprung weights G_{21} and G_{22} are as follows:

$$\sum X = z \cdot G_{21} - T_{21} + T_3\cos\alpha_1 = 0 \tag{47}$$

$$\sum Z = R_{21} + T_3\sin\alpha_1 - R_3 - R_{32} - G_{21} = 0 \tag{48}$$

$$\sum M_3 = -R_{32}c + R_{21}c_1 - G_{21}c_1 - z \cdot G_{21}(h_s - h_2) + T_{21}h_s - T_3\cos\alpha_1\,(h_s - h_{r1}) + T_3\sin\alpha_1\,(c_1 - c_{r1}) \tag{49}$$

$$\sum X = z \cdot G_{22} - T_{22} + T_4\cos\alpha_2 = 0 \tag{50}$$

$$\sum Z = R_{22} + T_4\sin\alpha_2 - R_4 - R_{42} - G_{22} = 0 \tag{51}$$

$$\sum M_4 = R_{42}c - R_{22}c_2 + G_{22}c_2 - z \cdot G_{22}(h_s - h_2) + T_{22}h_s - T_4\cos\alpha_2\,(h_s - h_{r2}) - T_4\sin\alpha_2\,(c_2 + c_{r2}) \tag{52}$$

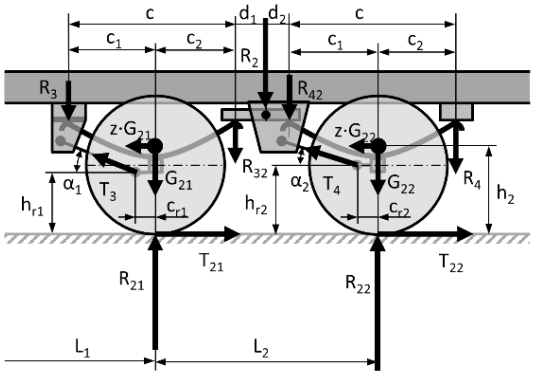

Fig. 6. Forces acting on a two leaf-two rod suspension

From equations (49) and (52), the reactions acting on the ends of the equalizer beam are given:

$$R_{32} = (R_{21} - G_{21})\frac{c_1}{c} - z \cdot G_{21}\frac{h_{r1} - h_2}{c} + T_{21}\frac{h_{r1}}{c} + (T_{21} - z \cdot G_{21})\tan\alpha_1\frac{c_1 - c_{r1}}{c} \tag{53}$$

$$R_{42} = (R_{22} - G_{22})\frac{c_2}{c} + z \cdot G_{22}\frac{h_{r2} - h_2}{c} - T_{22}\frac{h_{r2}}{c} + (T_{22} - z \cdot G_{22})\tan\alpha_2\frac{c_2 + c_{r2}}{c} \tag{54}$$

which are interrelated by the equation of force moments:

$$R_{32}d_1 = R_{42}d_2 \tag{55}$$

Solving equations (17), (18) and (53) - (54) together, the semi-trailer axle loads, and the coupling force are obtained:

$$R_1 = G - \frac{L_2}{MN}\Big\{[G[a - z(h - h_h)] - (T_{21} + T_{22})h_h]\,\frac{c_1(d_1 - d_2) + c \cdot d_2}{L_2} + G_{21}d_1[c_1 + z(h_{r1} - h_2)] - G_{22}d_2[c - c_1 - z(h_{r2} - h_2)] - (T_{21}d_1h_{r1} + T_{22}d_2h_{r2}) + ED\Big\} \tag{56}$$

$$R_{21} = \frac{L_1 + L_2}{MN}\Big\{[G[a - z(h - h_h)] - (T_{21} + T_{22})h_h]\,\frac{d_2(c - c_1)}{L_1 + L_2} + G_{21}d_1[c_1 + z(h_{r1} - h_2)] - G_{22}d_2[c - c_1 - z(h_{r2} - h_2)] - (T_{21}d_1h_{r1} + T_{22}d_2h_{r2}) + ED\Big\} \tag{57}$$

$$R_{22} = \frac{L_1}{MN}\Big\{[G[a - z(h - h_h)] - (T_{21} + T_{22})h_h]\,\frac{c_1d_1}{L_1} - G_{21}d_1[c_1 + z(h_{r1} - h_2)] + G_{22}d_2[c - c_1 - z(h_{r2} - h_2)] + (T_{21}d_1h_{r1} + T_{22}d_2h_{r2}) - ED\Big\} \tag{58}$$

where
$MN = d_2L_1c_2 + c_1d_1(L_1 + L_2)$ $\quad ED = (T_{22} - z \cdot G_{22})\tan\alpha_2\,d_2(c_2 + c_{r2}) - (T_{21} - z \cdot G_{21})\tan\alpha_1 d_1\,(c_1 - c_{r1})$

Equations (56) - (58) become much simpler when $\alpha_1 = \alpha_2 = 0$, since then ED = 0.

sciendo
DOI 10.2478/ama-2025-0012

3.4. Two leaf spring with equalization

A tandem double leaf spring suspension with equalization [4] has a pair of slipper springs and a mechanical equalisation of the braking load (Fig. 7). The rear end of the front spring is connected to the rear end of the rear spring by a rocker arm which is hinged to a central hanger bracket. This rocker distributes static (and shock) loads evenly between the two axles. An alternative design solution for a non-reactive tandem suspension with a bell crank and a tie-rod linkage is described in [5]. The forces acting on the two leaf spring suspensions with equalisation are presented in Fig. 7.

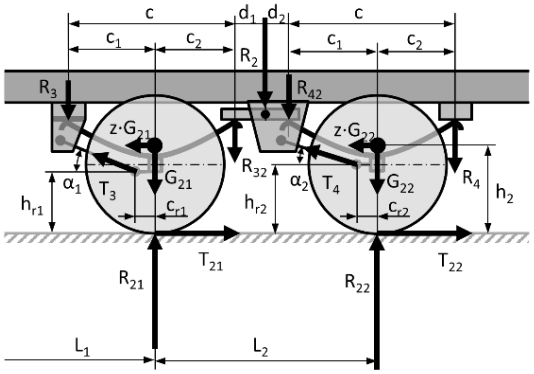

Fig. 7. Forces acting on two leaf spring suspension with equalization

The force and moment equations for the unsprung weights G_{21} and G_{22} of the suspension are given by:

$$\sum X = z \cdot G_{21} - T_{21} + T_3 = 0 \tag{59}$$

$$\sum Z = R_{21} - R_3 - R_{43} - G_{21} = 0 \tag{60}$$

$$\sum M_3 = -R_{43}c + R_{21}c_1 - G_{21}c_1 - z \cdot G_{21}(h_s - h_2) + T_{21}h_s = 0 \tag{61}$$

$$\sum X = z \cdot G_{22} - T_{22} + T_2 = 0 \tag{62}$$

$$\sum Z = R_{22} - R_2 - R_{42} - G_{22} = 0 \tag{63}$$

$$\sum M_4 = -R_{42}c + R_{22}c_1 - G_{22}c_1 - z \cdot G_{22}(h_s - h_2) + T_{22}h_s = 0 \tag{64}$$

Equations (61) and (64) are used to compute the reactions at the ends of the beam:

$$R_{43} = (R_{21} - G_{21})\frac{c_1}{c} - z \cdot G_{21}\frac{h_s - h_2}{c} + T_{21}\frac{h_s}{c} \tag{65}$$

$$R_{42} = (R_{22} - G_{22})\frac{c_1}{c} - z \cdot G_{22}\frac{h_s - h_2}{c} + T_{22}\frac{h_s}{c} \tag{66}$$

related by the equation of moments:

$$R_{43}d_1 = R_{42}d_2 \tag{67}$$

By solving the system of equations (17), (18), (65) – (67), the vertical coupling force and the dynamic axle loads are obtained during deceleration of the semi-trailer:

$$R_1 = \frac{1}{c_1 L}\{G[L - a + z(h - h_h)]c_1 + (T_{21} + T_{22})h_h c_1 - (G_{21}d_1 - G_{22}d_2)[c_1 + z(h_s - h_2)] + (T_{21}d_1 - T_{22}d_2)h_s\} \tag{68}$$

$$R_{21} = \frac{1}{c_1 L}\left\{G[a + z(h - h_h)]\frac{c_1 d_2}{L_2} - (T_{21} + T_{22})h_h\frac{c_1 d_2}{L_2} + \frac{L_1 + L_2}{L_2}(G_{21}d_1 - G_{22}d_2)[c_1 + z(h_s - h_2)] - \frac{L_1 + L_2}{L_2}(T_{21}d_1 - T_{22}d_2)h_s\right\} \tag{69}$$

$$R_{22} = \frac{1}{c_1 L}\left\{G[a + z(h - h_h)]\frac{c_1 d_1}{L_2} - (T_{21} + T_{22})h_h\frac{c_1 d_1}{L_2} - \frac{L_1}{L_2}(G_{21}d_1 - G_{22}d_2)[c_1 + z(h_s - h_2)] + \frac{L_1}{L_2}(T_{21}d_1 - T_{22}d_2)h_s\right\} \tag{70}$$

where: $L_2 = d_1 + d_2$ and $L = L_1 + d_1$.

3.5. Air suspension

With air suspension, the air springs are mounted to the trailing arms via a crossmember and attached to the frame at the top (Fig. 8). The trailing arms are hinged to the hanger brackets and axle housings. All the air bags are connected by air lines to balance the axle loads. Vertical forces are distributed between the hanger brackets and the airbags. Longitudinal forces from braking are transferred to the trailer frame through the hanger brackets.

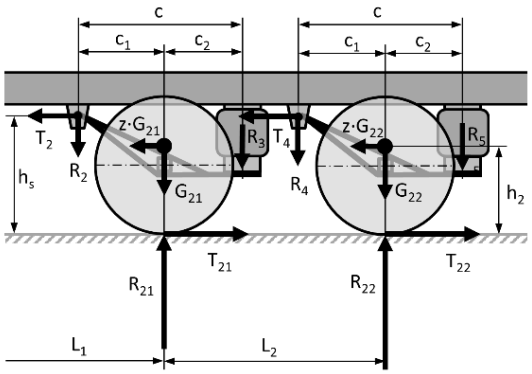

Fig. 8. Forces acting on air tandem suspension

The balance equations for the forces and moments applied to the suspension with unsprung weights G_{21} and G_{22} are calculated as follows:

$$\sum X = z \cdot G_{21} - T_{21} + T_2 = 0 \tag{71}$$

$$\sum Z = R_{21} - R_2 - R_3 - G_{21} = 0 \tag{72}$$

$$\sum M_3 = -R_3 c + R_{21}c_1 - G_{21}c_1 - z \cdot G_{21}(h_s - h_2) + T_{21}h_s = 0 \tag{73}$$

$$\sum X = z \cdot G_{22} - T_{22} + T_4 = 0 \tag{74}$$

$$\sum Z = R_{22} - R_4 - R_5 - G_{22} = 0 \tag{75}$$

$$\sum M_4 = -R_5 c + R_{22}c_1 - G_{22}c_1 - z \cdot G_{22}(h_s - h_2) + T_{22}h_s = 0 \tag{76}$$

On the assumption that the pressure in the airbags is the same, the vertical reactions transmitted by the air springs will be the same as well: R_3=R_5. Then from equations (73) and (76), where G_{21}=G_{22}, the relationship between the loads of the tandem axles is obtained:

$$R_{21}c_1 + T_{21}h_s = R_{22}c_1 + T_{22}h_s \tag{77}$$

The solution of the system of equations (17), (18) and (77) is the vertical coupling force and the trailer axle loads:

DOI 10.2478/ama-2025-0012

$$R_1 = \frac{G}{L}[L - a + z(h - h_h)] + (T_{21} + T_{22})\frac{h_h}{L} + \frac{L_2}{L}(T_{21} - T_{22})\frac{h_s}{2c_1} \quad (78)$$

$$R_{21} = \frac{G}{2L}[a - z(h - h_h)] - (T_{21} + T_{22})\frac{h_h}{2L} - \frac{L_1+L_2}{L}(T_{21} - T_{22})\frac{h_s}{2c_1} \quad (79)$$

$$R_{22} = \frac{G}{2L}[a - z(h - h_h)] - (T_{21} + T_{22})\frac{h_h}{2L} + \frac{L_1}{L}(T_{21} - T_{22})\frac{h_s}{2c_1} \quad (80)$$

where: $L = L_1 + L_2/2$.

4. BRAKING OF SEMI-TRAILERS WITH TANDEM SUSPENSION

As proved in section 2, the ideal braking condition for semi-trailers is achieved when the rate of utilized adhesion of each axle and the quotient of the horizontal to vertical force at the coupling is equal to the braking rate z of the combination. For semi-trailers with a single or tandem axle, this condition can be expressed as follows:

$$f_1 = f_2 = f_{2i} = z \qquad z = \frac{T_1 + \sum T_{2i}}{R_1 + \sum R_{2i}} \quad (81)$$

where T_1, R_1 – braking force and normal reaction on the coupling device, T_{2i} , R_{2i} – braking forces and normal loads on tandem axle, i – axle number in the tandem unit.

The adhesion utilization rates used by the front coupling and the rear axle assembly are calculated based on the relationship:

$$f_1 = \frac{T_1}{R_1} \qquad f_2 = \frac{\sum f_{2i} R_{2i}}{\sum R_{2i}} \quad (82)$$

With ideal braking, stopping distance is minimised and braking efficiency requirements are met with reserve (z≥50% at 6.5 bar pressure) as each axle reaches its maximum braking force capability [40].

Due to varying trailer loads, it is virtually impossible to ensure ideal brake distribution, even with the application of brake force regulators. Therefore, for agricultural trailers travelling at speeds above 40 km/h, acceptable limits have been set for the deviation of the adhesion utilisation rates of individual axles from the optimal distribution. When considering brake force distribution, each part of the combination is deemed to be a single vehicle without considering the force at the coupling. The UE regulation allows for two solutions, as shown in Fig. 9 [8].

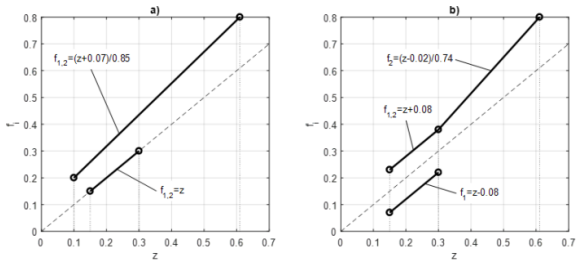

Fig. 9. Limits of adhesion utilization in accordance with Commission Delegated Regulation (EU) 2015/68 [8]: a – first solution, b – second solution

The first solution: the adhesion utilization rate for each axle group must satisfy the condition of ensuring the minimum required braking performance:

$$f_{1,2} \le \frac{z+0.07}{0.85} \quad \text{when} \quad 0.1 \le z \le 0.61 \quad (83)$$

and the condition of prior locking of the wheels of the front axle to ensure straight-ahead stability:

$$f_1 > z > f_2 \quad \text{when} \quad 0.15 \le z \le 0.30 \quad (84)$$

Second solution: the axle adhesion utilization rates should be within a certain range, then the wheel locking limits are established by the following relationships:

$$\begin{matrix} f_1 \ge z - 0.08 \\ f_{1,2} \le z + 0.08 \end{matrix} \quad \text{when} \quad 0.15 \le z \le 0.30 \quad (85)$$

Furthermore, the adhesion curve for the rear axle assembly should satisfy the requirement:

$$f_2 \le \frac{z-0.02}{0.74} \quad \text{when} \quad 0.30 \le z \le 0.61 \quad (86)$$

For accurate calculations, the divisor in inequality (86) should be set to 0.7381.

The requirements concerning the wheel locking sequence are met if the adhesion utilized by the front axle is greater than that utilized by at least one of the rear axles at braking rates between 0.15 and 0.30 [8]:

$$f_1 > f_{2i} \quad \text{for any } i \quad (87)$$

Of course, in the case of the application of these solutions for a semi-trailer, the requirements for the front axle relate to the coupling device.

5. METHOD OF SELECTION OF LINEAR BRAKE FORCE DISTRIBUTION

In the air braking systems of agricultural trailers, various types of load-dependent brake force regulators are used to approximate the ideal brake force distribution. The automatic load-sensing valves (LSVs) currently fitted to heavy trailers are designed to adjust the brake pressure on the axles according to the load condition [41]. If the braking forces are designed correctly, this will prevent the wheels from locking when the vehicle is unladen or only partially laden. On mechanically suspended trailers, the regulation is proportional to the spring deflection, while on air-suspended trailers, it depends on the control pressure of the air springs. If there are technical reasons against equipping the vehicles with an LSV (especially unsuspended vehicles), agricultural trailers or machines should be equipped with a manual brake force regulator. In the most popular three-stage adjustment device (full - half - empty), the regulation of braking force is achieved by pressure limitation in axle brake chambers [41]. Due to the difficulty to comply with the requirements of EU 2015/68 for the distribution of braking forces on vehicles with manual regulators, which were mentioned before, BPW developed a seven-position mechanical load-dependent brake force regulator (MBL), but with linear characteristics [42]. The BPW MLB works with a proportional pressure control. As a result, the output pressure remains proportional to the control pressure. This kind of control fully complies with the requirements of the EU regulation for unsuspended vehicles.

As the pressure distribution characteristic of the ALB and MLB

DOI 10.2478/ama-2025-0012

is essentially a straight line, the distribution of braking forces between the coupling device and the rear axles can also be regarded as linear (radial). The contribution of the coupling device and trailer axles to the braking of the semi-trailer is expressed by the ratio of the partial braking force on the coupling device or individual axle to the total braking force:

$$\beta_1 = \frac{T_1}{z \cdot G} \quad \beta_2 = \frac{T_{2T}}{z \cdot G} \quad \beta_{21} = \frac{T_{21}}{z \cdot G} \quad \beta_{22} = \frac{T_{22}}{z \cdot G} \tag{88}$$

where: T_{2T} – total braking force of the tandem axles.

The values of the braking force distribution coefficients defined in this way can theoretically vary from 0 to 1 and satisfy the following relationships:

$$\beta_1 + \beta_2 = 1 \qquad \beta_{21} + \beta_{22} = \beta_2 \tag{89}$$

Using the relations (88) and (89), the braking force of the coupling device and trailer axles can be calculated:

$$T_1 = \beta_1 z \cdot G \qquad T_{2T} = (1 - \beta_1) z \cdot G \qquad T_{21} = \beta_{21} z \cdot G$$
$$T_{22} = (1 - \beta_1 - \beta_{21}) z \cdot G \tag{90}$$

A directional coefficient of the brake distribution line, which passes through the origin of the coordinate system $T_{2T} = f(T_1)$, is calculated as follows:

$$i_P = \frac{T_{21} + T_{22}}{T_1} = \frac{T_{2T}}{T_1} \tag{91}$$

Similarly, a linear braking force distribution, variable or fixed (in the absence of a braking force regulator), can be applied to the tandem assembly:

$$i_S = \frac{T_{22}}{T_{21}} \tag{92}$$

Unlike the β coefficients, the values of the i_P and i_S ratios can theoretically range from zero to infinity, especially when the braking force of one axle is close to zero.

To find optimal solutions for the linear brake force distribution, the Quasi Monte Carlo method [43-45] was chosen. Fig. 10 shows an example block diagram of the algorithm for the optimum selection of the braking force distribution coefficients β_1 and β_{21}.

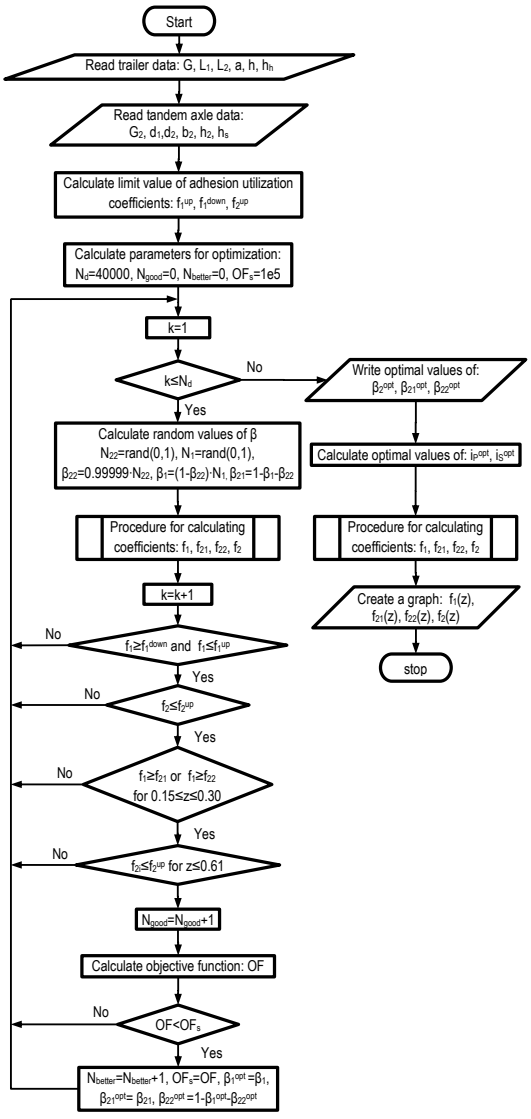

Fig. 10. A block diagram of an algorithm for the optimization of brake forces of a semi-trailer with tandem suspension using the Monte Carlo method (OF_s – initial value of the objective function, N_d – number of draws, N_{good} – number of good solutions, meeting inequality constraints, N_{better} – number of better solutions, reducing the value of the objective function)

DOI 10.2478/ama-2025-0012

The optimal values of the brake force distribution coefficients are determined by minimizing the objective function consisting of the residual sum of squares:

$$OF = \frac{w_1(f_1-f_2)^2+w_2(f_{21}-f_{22})^2}{w_1+w_2} \quad (93)$$

where: w_i – weighting factors.

The OF thus obtained favourable solutions with the smallest differences between the adhesion utilised by each axle. As it is more important to reduce the difference between the values f_1 and f_2 than to reduce the difference between the adhesion values f_{21} and f_{22} utilised by the rear axles to fulfil the requirements (83) - (86), $w_1 > w_2$ should, therefore, be taken in the OF criterion.

Before the computation of the OF, the inequality conditions (83), (84) for the first solution and (85), (86) for the second solution are checked:

$$f_1^{up} \geq f_1 = \frac{T_1}{R_1} \geq f_1^{down} \qquad f_2 = \frac{T_{21}+T_{22}}{R_{21}+R_{22}} \leq f_2^{up} \quad (94)$$

To simplify the notation of the boundary equations, they have been expressed as the product of the algebraic and logical equations. For the first solution:

$$f_1^{down} = z \cdot (0.15 \leq z \leq 0.30) \quad (95)$$

$$f_1^{up} = f_2^{up} = (z + 0.07)/0.85 \cdot (0.10 \leq z \leq 0.61) \quad (96)$$

For the second solution:

$$f_1^{down} = (z - 0.08) \cdot (0.15 \leq z \leq 0.30) \quad (97)$$

$$f_1^{up} = (z + 0.08) \cdot (0.15 \leq z \leq 0.30) \quad (98)$$

$$f_2^{up} = (z + 0.08) \cdot (0.15 \leq z \leq 0.30) + \left(\frac{z-0.3}{0.7381} + 0.36\right) \cdot (0.3 < z \leq 0.61) \quad (99)$$

Then, the condition (87) for multi-axle trailer is checked:

$$f_1 > f_{21} \quad \text{or} \quad f_1 > f_{22} \quad \text{for} \quad z = 0.15 \div 0.30 \quad (100)$$

In addition, an extra condition has been added to the rear axle adhesion utilisation rates:

$$f_{2i} \leq f_2^{up} \quad \text{for} \quad z \leq 0.61 \quad (101)$$

which limits the unduly high increase of the coefficient f_{22} for $z \leq 0.61$.

6. RESULTS OF OPTIMIZATION CALCULATIONS

Based on the algorithm described above, a computer program was written in MATLAB [46] to calculate the optimum distribution of the braking forces for semi-trailers with tandem suspension. The same algorithm, but without calculating the coefficients f_{21} and f_{22}, was used to calculate the single-axle semi-trailer. The MATLAB procedure of the Hammersley sequence [47] by Burkardt [48] was used to generate the quasi-random numbers N_{22} and N_1 (Fig. 10). The two-dimensional Hammersley point set is one of the simplest sequences with a low discrepancy that is used in both numerical and graphical applications [49]. The number of draws has been set to Nd = 40.000. The OFs (93) were calculated for the following values of the weighting factors $w_1=0.6$, $w_2=0.4$ in the range $0.1 \leq z \leq 0.66$ with a step size of 0.01.

The technical data and calculation results of the brake force distribution for the laden and unladen single axle semi-trailer are shown in Tab. 1.

Tab. 1. The technical data and results of the optimization of brake force distribution in single axle semi-trailer: L_1=4.45 m, h_h=0.7 m (L – laden, U – unladen, I, II – first and second solution)

	m kg]	a [m]	h [m]	OF	β_1	i_P
U_I-U_{II}	2250	3.895	0.98	0.0947-0.0947	0.2079-0.2079	3.8097-3.8097
L_I - L_{II}	7250	3.840	1.25	0.1272-0.1272	0.2445-0.2445	3.0901-3.0901

In the case of laden and unladen semi-trailers, identical results were obtained for the optimum distribution of braking forces using both solutions. The adhesion utilization curves of the braked axle and the trailer coupling are shown in Fig. 11.

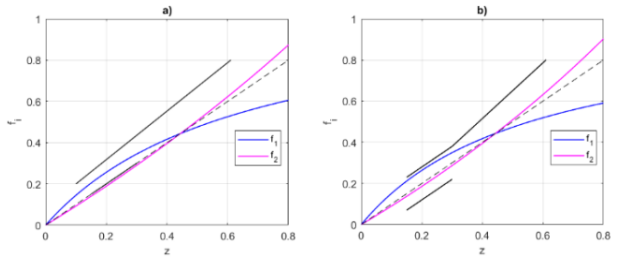

Fig. 11. Adhesion utilization curves fi(z) for an optimal distribution of brake forces in a single axle semi-trailer: a – an unladen trailer (I solution), b – a laden trailer (II solution)

The technical data of the laden and unladen semi-trailer with different tandem suspensions taken for the optimization calculations are presented in Tab. 2. To achieve comparability of the calculation results, the same mass m_2=1700 kg was taken for all types of suspensions, and some geometrical parameters of suspensions obtained from literature data [37-38] were fixed. In addition, no changes were made to some of the suspension dimensions for the laden and unladen trailers. Based on the calculated results of the β_1, β_{21}, β_{22}, i_P and i_S ratios presented in Tab. 3, the braking force distribution in a tandem semi-trailer depends significantly on the trailer load and the type of tandem suspension.

Following the optimization criterion used (lowest OF values), the air suspension (section 3.5) and the two leaf spring suspensions with equalization (section 3.4) can be regarded as the best. The same optimum brake force distribution ratios were found for these tandem suspensions (Table 3) using the solutions described in Section 2. The values after the dash have been obtained by considering the weight of the tandem axle. Moreover, with equalised values of the β_{21} and β_{22} coefficients (the values of the i_S coefficients are close to 1), the trailer with these suspensions has a uniform, close to ideal, distribution of the braking forces. Therefore, the adhesion utilization curves f_{21}, f_{22} and f_2 almost coincide (Fig. 12-a, c).

DOI 10.2478/ama-2025-0012

Tab. 2. Rigid drawbar trailer and tandem suspension technical data [37-38]

Semi-trailer with tandem axle		**Tandem suspension**				
unladen	laden	bogie (3.1)	2 leaf spring (3.2)	2 leaf 2 rod (3.3)	2 leaf equal. (3.4)	air susp. (3.5)
m=3900 kg	m=19800 kg	d_1=0.705 m	c_1=0.454 m	c1=0.497 m	c1=0.454 m	c1=0.5 m
L_1=3.94 m	L_1=3.94 m	d_2=0.645 m	c=0.93 m	c=0.97 m	c=0.93 m	c=0.88 m
L_2=1.35 m	L_2=1.35 m	h_s=0.567 m	h_s=0.717 m	h_{r1}=h_{r1}=0.467 m	h_s=0.717 m	hs=0.717 m
a=4.26 m	a=4.055 m	h_2=0.547 m	h_2=0.567 m	h_2=0.567 m	h_2=0.567 m	h_2=0.567 m
h=1.19 m	h=1.62 m	b_2=0.03 m	d_1=d_2=0.21m	d_1=d_2=0.19 m	d_1=d_2=0.675 m	
h_h=0.59 m	h_h=0.59 m			α_1= α_2=15°		

Tab. 3. The results of the optimization of brake force distribution in a tandem axle semi-trailer (L –laden, U – unladen, L_w, U_w – laden and unladen with weight of suspension)

Suspension		**OF**	**β_1**	**β_{21}**	**β_{22}**	**i_P**	**i_S**
Bogie (3.1)	U-U_w	0.3040-0.3115	0.1629-0.1588	0.5740-0.5793	0.2631-0.2619	5.1402-5.2971	0.4583-0.4521
I and II solution	L-L_w	0.3006-0.3015	0.2301-0.2301	0.5286-0.5286	0.2412-0.2412	3.3456-3.3456	0.4564-0.4564
2 leaf 2 rod (3.3)	U-U_w	0.6716-0.8831	0.2313-0.2307	0.1803-0.1527	0.5884-0.6166	3.3239-3.3354	3.2635-4.0377
I solution	L-L_w	0.5841-0.6991	0.3117-0.3267	0.1674-0.1644	0.5209-0.5189	2.2086-2.1574	3.1116-3.1573
II solution	U-U_w	0.9446-1.2169	0.2075-0.2065	0.1705-0.1444	0.6220-0.6490	3.8198-3.8417	3.6483-4.4935
	L-L_w	0.7531-0.7893	0.2806-0.2818	0.1577-0.1525	0.5617-0.5657	2.5635-2.5490	3.5631-3.7096
2 leaf equal. (3.4)	U-U_w	0.2512-0.2512	0.1951-0.1951	0.4031-0.4031	0.4018-0.4018	4.1265-4.1265	0.9969-0.9969
I solution	L-L_w	0.2099-0.2099	0.2605-0.2605	0.3710-0.3710	0.3685-0.3685	2.8388-2.8388	0.9935-0.9935
II solution	U-U_w	0.3002-0.3002	0.1803-0.1803	0.4040-0.4040	0.4156-0.4156	4.5449-4.5449	1.0288-1.0288
	L-L_w	0.2117-0.2117	0.2561-0.2561	0.3721-0.3721	0.3717-0.3717	2.9046-2.9046	0.9989-0.9989
air susp. (3.5)	U-U_w	0.2511-0.2511	0.1951-0.1951	0.4031-0.4031	0.4018-0.4018	4.1265-4.1265	0.9969-0.9969
I solution	L-L_w	0.2098-0.2098	0.2605-0.2605	0.3710-0.3710	0.3685-0.3685	2.8388-2.8388	0.9935-0.9935
II solution	U-U_w	0.3003-0.3003	0.1803-0.1803	0.4040-0.4040	0.4156-0.4156	4.5449-4.5449	1.0288-1.0288
	L-L_w	0.2117-0.2117	0.2561-0.2561	0.3721-0.3721	0.3717-0.3717	2.9046-2.9046	0.9989-0.9989
2 leaf (3.2) only	U-U_w	5.3013-3.5221	0.2271-0.2337	0.0017-0.0218	0.7712-0.7446	3.4025-3.2798	458.23-34.199
I solution	L-L_w	4.6761-4.5855	0.3230-0.3202	0.0018-0.0030	0.6752-0.6768	2.0957-2.1233	376.30-222.04

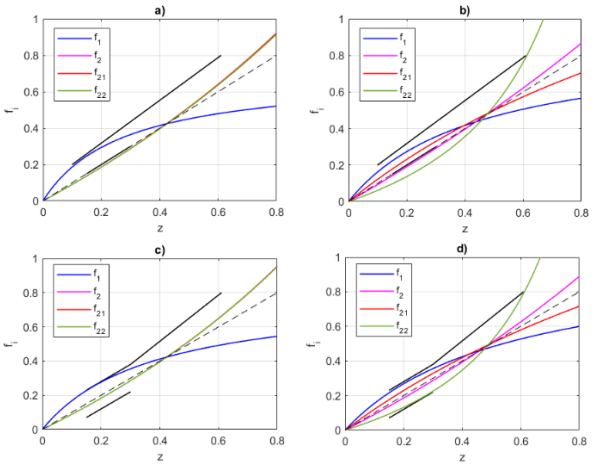

Fig. 12. Adhesion utilization curves fi*(z)* for an optimal distribution of brake forces in a tandem semi-trailer (considering the weight of the tandem suspension): a – an unladen trailer with air suspension (I solution), c – a laden trailer with air suspension (II solution), b – an unladen trailer with bogie suspension (I solution), d – a laden trailer with bogie suspension (II solution)

Larger values of the OF were obtained for the bogie suspension (section 3.1) and even higher values for the two leaf-two rod suspension (section 3.3). In both cases, this causes a greater deviation of the adhesion utilization curves from the ideal distribution of braking forces (Fig. 12-b, d and Fig.13-a, c).

For the two-leaf suspension (section 3.2), the calculation of the distribution of braking forces was only obtained from the first solution, with values of the OF objective function an order of magnitude higher (from 3.5 to 5.3) than for the other tandem suspensions. However, this solution cannot be considered correct either, as the leading tandem axle is braked to a very small extent (β_{21} values range from 0.003 to 0.022 - Table 3). In addition, once the z-value exceeds 0.6, the wheels of this axle start to come off the ground (the f_{21} values go to infinity and then fall below zero - Fig.13-b, d). Thus, f_i curves for braking rates above 0.6 make no physical sense. Braking at very low vertical loads can, according to the literature [3, 4], cause wheel lock on the leading axle. It should be noted that qualitatively similar results were obtained when calculating the braking force distribution on three-axle trailers with tandem axles [33].

DOI 10.2478/ama-2025-0012

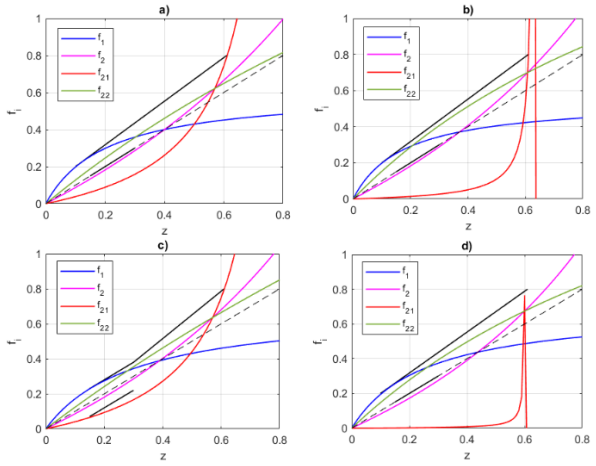

Fig. 13. Adhesion utilization curves $f_i(z)$ for an optimal distribution of brake forces in a tandem axle semi-trailer (considering the weight of the tandem suspension): a – an unladen trailer with two leaf-two rod suspension (I solution), c – a laden trailer with two leaf-two rod suspension (II solution), b – an unladen trailer with two leaf suspension (I solution), d – a laden trailer with two leaf suspension (I solution)

A comparison of the results obtained without and with the weight of the tandem shows that for most tandems, the effect of this weight on the distribution of braking forces has been negligible. The differences in the brake force distribution ratios are no more than 5%. But for suspension 3.3, the differences in the calculated values of the β_{21} ratio are about 18%, and for suspension 3.2, they are even up to 92%. Omitting the weight of the tandem suspension in the calculation of the braking force distribution considerably simplifies the relationships for the vertical reactions of the braked axles and, above all, avoids the many time-consuming steps over determining the mass of the tandem suspension and the position of its centre of gravity.

7. SUMMARY AND CONCLUSIONS

The method described for optimising the choice of linear brake force distribution for rigid drawbar agricultural trailers with single and tandem axles can be used in the initial design phase of air braking systems using the ALB or MLB regulator with radial characteristic. The calculation of the braking force distribution considered the requirements of EU Directive 2015/68 [8] for multi-axle trailers, treating the coupling device of a rigid drawbar trailer as a contractual front axle. It should be noted that although optimising the brake force distribution improves the braking performance and directional stability of agricultural vehicle combinations on different road surfaces, it does not prevent individual wheels from lockup, particularly on slippery and uneven surfaces. Therefore, agricultural vehicles travelling at speeds above 60 km/h must be equipped with ABS systems [8].

Optimization calculations using the Quasi Monte Carlo method for a rigid drawbar trailer with a payload of approximately 16 tonnes showed that the distribution of braking forces depends significantly on the type of tandem suspension. The lowest values of the minimized objective function were obtained for tandem axles with air suspension and two leaf springs suspension with equalization. For these two tandem assembly, the adhesion utilizations of the individual axles are closest to the straight line representing the ideal brake force distribution (Fig. 12-a,c), where the adhesion utilized by each tandem axle is the same and equal to the braking rate. Higher values of OF were found for the bogie suspension (Fig. 12-b, d), and even higher for the two leaf-two rod suspension (Fig. 13-a, c). In both cases, this leads to a greater deviation of the adhesion utilisation curves from the ideal distribution of the braking forces. The two leaf spring suspension (Figure 13-b, d) produced the highest OF values. These results are in qualitative agreement with Limpert's analysis of the braking dynamics of a vehicle combination with tandem axles [4]. In addition, calculations for the two leaf spring suspension have shown that the load transfer between the tandem axles can lead to premature locking of the leading axle wheels at a braking rate of about 0.6, which is also confirmed in the literature [3, 4]. The results of the optimisation calculations show that for most tandem suspensions, the effect of the suspension mass on the brake force distribution is negligible.

REFERENCES

1. Revised standards for agricultural vehicles. RSA Guide. Road Safety Authority; 2015. Available from: https://www.rsa.ie/docs/default-source/road-safety/r1.6-agricultural-vehicles/revised-standards-for-agricultural-vehicles.pdf?Status=Master&sfvrsn=670b2fb7_5
2. Gillmann R. Axle Spacing and Load Equivalency Factors. Transportation Research Record 1998;(1655):227–232. https://doi.org/10.3141/1655-29.
3. Harwood DW. Review of truck characteristics as factors in roadway design. The National Academies Press; 2003. https://doi.org/10.17226/23379
4. Limpert R. Brake design and safety. SAE International, 2011. https://doi.org/10.4271/R-398
5. Heisler H. Advanced vehicle technology. Elsevier, 2002. https://doi.org/10.1016/b978-0-7506-5131-8.x5000-3
6. Nunney MJ. Light and heavy vehicle technology. Elsevier; 2007. https://doi.org/10.4324/9780080465753
7. Van Straelen B. Lastverlagerung und Bremskraftverteilung bei Einachs- und Doppelachsanhängern. Grundlagen Der Landtechnik 1983; 33(6): 183–189.
8. Commission Delegated Regulation (EU) 2015/68 of 15 October 2014 Supplementing Regulation (EU) No 167/2013 of the European Parliament and of the Council with Regard to Vehicle Braking Requirements for the Approval of Agricultural and Forestry Vehicles.
9. ECE Regulation No. 13. Uniform Provisions Concerning the Approval of Vehicles of Categories M, N and O with Regard to Braking. UN Economic Commission for Europe; Switzerland 2001.
10. Radlinski R, Flick M. Tractor and trailer brake system compatibility. SAE Technical Paper 861942; 1986. https://doi.org/10.4271/861942
11. Glišović J, Lukić J, Šušteršič V, Ćatić D. 2015. Development of tractors and trailers in accordance with the requirements of legal regulations. In: Proc. of 9th International Quality Conference. Kragujevac, Serbia 2015; 193–202.
12. Nastasoiu M, Ispas N. Comparative analysis into the tractor-trailer braking dynamics: tractor with single axle brakes, tractor with all wheel brakes. Central European Journal of Engineering 2014; 4(2): 142–147. https://doi.org/10.2478/s13531-013-0155-0
13. Janulevičius A, Giedra K. The evaluation of braking efficiency of tractor transport aggregate. Transport 2002; 17(4): 152-158. https://doi.org/10.3846/16483840.2002.10414033
14. Aykan H, Çarman K, Canlı E, Ekinci Ş. Evaluation of tractor-trailer combination braking performance in different operating conditions. Journal of Natural and Applied Sciences. 2023; 27(2): 219-25.
15. Abu-Hamdeh NH. Stability and computer simulation of trailed implement under different operating conditions. Applied Mechanics and Materials. 2016; 826 :61–5. https://doi.org/10.4028/www.scientific.net/amm.826.61

16. Bădescu M, Iordache S, Ivancu B, Persu C, Bunduchi G, Epure M, Vlăduţ V. Theoretical study of the system of forces and moments acting on tractor-semitrailer aggregate, into rectilinear motion. Annals of the Faculty of Engineering Hunedoara - International Journal of Engineering 2014; 12(3): 221-228.
17. Popescu S, Candea I, Csatlos C. Influence of the tractor and semitrailer mass ratio on braking stability. Commission of Motorization and Power Industry in Agriculture 2004; 4: 7-13.
18. Ogunjirin OA, Ogunlela AO. An appraisal of safety of tractor-trailer braking system. Nigerian Journal of Technological Development. 2011; 8(1): 10-22.
19. Ciuperca R, Popa L, Nedelcu A, Borisov B, Atanasov A. Braking of trailer endowed with inertial braking system, working in aggregate with tractor. INMATEH Agricultural Engineering. 2010;32(3): 51-58.
20. Ahokas J, Kosonen S. Dynamic behaviour of a tractor-trailer combination during braking. Biosystems Engineering. 2002; 85(1): 29–39. https://doi.org/10.1016/S1537-5110(03)00035-7
21. Dwyer MJ. The braking performance of tractor-trailer combinations. Journal of Agricultural Engineering Research. 1970; 15(2): 148–162. https://doi.org/10.1016/0021-8634(70)90086-7
22. Pierce P. Controlled load transfer during braking on a four-spring trailer suspension. SAE Technical Paper 85234; 1985. https://doi.org/10.4271/852344
23. Mital A, Desai A, Subramanian A, Mital A. Product development: A structured approach to consumer product development, design, and manufacture. Elsevier Science; 2014. https://doi.org/10.1016/B978-0-12-799945-6.00015-6
24. Goodarzi A, Mehrmashhadi J, Esmailzadeh E. Optimised braking force distribution strategies for straight and curved braking. International Journal of Heavy Vehicle Systems IJHVS. 2009; 16(1); 78-89. https://doi.org/10.1504/IJHVS.2009.023856
25. Zhang N, Wu J, Li T, Zhao Z, Yin G. Influence of braking on dynamic stability of car-trailer combinations. Proceedings of the Institution of Mechanical Engineers, Part D: Journal of Automobile Engineering 2021; 235(2-3): 455-464. https://doi.org/10.1177/09544070209598
26. Limpert R. An investigation of the brake force distribution on tractor-semitrailer combinations. SAE Technical Paper 710044; 1971. https://doi.org/10.4271/710044
27. Nakazawa M, Isobe O, Takahashi S, Watanabe Y. Braking force distribution control for improved vehicle dynamics and brake performance. Vehicle System Dynamics. 1995;24(4-5):413-426. https://doi.org/10.1080/00423119508969101
28. Nakazawa M, Isobe O, Takahashi S, Watanabe Y. Braking force distribution control for improved vehicle dynamics and brake performance. Vehicle System Dynamics. 1995;24(4-5):413-426. https://doi.org/10.1080/00423119508969101
29. Zheng H, Liu Z, Xu W. Braking force distribution strategy for comfort of tractor and semi-trailer combination. In: Proc. of the 2012 International Conference on Automobile and Traffic Science Materials, Metallurgy Engineering. Wuhan China 2012; 0108-0112. https://doi.org/10.2991/mmat.2013.21
30. Beyer C, Schramm H, Wrede J. Electronic braking System EBS - status and advanced functions. SAE Technical Paper 982781; 1998. https://doi.org/10.4271/982781
31. Kamiński Z, Radzajewski P. Calculations of the optimal distribution of brake force in agricultural vehicles categories R3 and R4. Eksploatacja i Niezawodność - Maintenance and Reliability. 2019; 21(4): 645–653. https://doi.org/10.17531/ein.2019.4.14
32. Miatluk M, Kaminski Z. Brake Systems of Road Vehicles. Calculations. Wydawnictwo Politechniki Bialostockiej; 2005.
Kamiński Z. Calculation of the optimal braking force distribution in three-axle trailers with tandem suspension. Acta Mechanica et Automatica. Sciendo. 2022;16(3):189-199. https://doi.org/10.2478/ama-2022-0023
33. Tang G, Zhao H, Wu J, Zhang Y. Optimization of braking force distribution for three-axle Truck. SAE Technical Paper; 2013. https://doi.org/10.4271/2013-01-0414
34. ISO 8855: 2011. Road vehicles - vehicle dynamics and road-holding ability - vocabulary.
35. Bryant D, Day A. Braking of road vehicles. Elsevier; 2022. https://doi.org/10.1016/C2019-0-04185-4
36. BPW. Agriculture equipment brochure; 2015. Available from: http://www.bpwtranspec.com.au/wp-content/uploads/2013/03/BPW_Agriculture_Equipment_brochure.pdf
37. Colaert Essieux. General catalogue; 2023. Available from: https://www.adraxles.com/gallery/catalogue-colaert-essieux-2023-v22-11-18-lr.pdf
38. Titan agricultural catalogue – tires, wheels, tracks, axles; 2015. Available from: http://titanaust.com.au/wp-content/uploads/2015/10/TITA0053-C1L3P2-Agricultural-Catalogue-COMPLETE_LR.pdf
39. NHTSA Heavy duty vehicle brake research program: Report no. 1 – Stopping capability of air braked vehicles. National Highway Traffic Safety Administration; 1985.
Available from: https://books.google.pl/books?id=pfbZvgEACAAJ
40. Pneumatic braking system. Agriculture and forestry. Product catalogue. Wabco; 2017. Available from: https://www.wabco-customercentre.com/catalog/docs/8150100823.pdf
41. BPW. Mechanical load-dependent brake force regulator. The unique solution for the requirements imposed by Regulation EU 2015/68. Available from: https://bpwagrar.comen/mlb/
42. Dimov IT. Monte Carlo methods for applied scientists. World Scientific Publishing Co; 2007. https://doi.org/10.1142/2813
43. Kroese DP, Taimre T, Botev ZI. Handbook of Monte Carlo methods. John Wiley & Sons; 2011. https://doi.org/10.1002/9781118014967
44. Morton DP, Popova E. Monte-Carlo simulations for stochastic optimization. In: Encyclopedia of Optimization. Springer; 2001. https://doi.org/10.1007/0-306-48332-7_305
45. Venkataraman P. Applied optimization with MATLAB programming. John Wiley & Sons, Inc.; 2009.
46. Hammersley J.M. Monte Carlo methods for solving multivariable problems. Annals of the New York Academy of Sciences. 1960; 86(3): 844-874. https://doi.org/10.1111/j.1749-6632.1960.tb42846.x
47. Burkhardt J. Various software. MATLAB source codes. The Hammersley Quasi Monte Carlo (QMC) sequence 2020. Available from: https://people.sc.fsu.edu/~jburkardt/ m_src/hammersley/hamm ersley.html
48. Wong TT, Luk WS, Heng PA. Sampling with Hammersley and Halton points. Journal of Graphics Tools. 2012; 2(2): 9-24. https://doi.org/10.1080/10867651.1997.10487471

Acknowledgements: This research was funded through a subsidy from the Ministry of Science and Higher Education of Poland, for the discipline of mechanical engineering at the Faculty of Mechanical Engineering at Bialystok University of Technology (WZ/WM-IIM/5/2023).

Zbigniew Kamiński: https://orcid.org/0000-0003-2693-5077